

JACoP: Joint Alignment for Compliant Multi-Agent Prediction

Supplementary Material

001 Section A details our sampling algorithm for generating
002 scene predictions via prototype alignment. Section B de-
003 fines the evaluation metrics used in our benchmark experi-
004 ments. Section C provide an additional benchmark on the
005 average ADE/FDE and KDE NLL metrics, highlighting JA-
006 CoP’s ability to produce predictions that are tightly concen-
007 trated around the ground-truth future and better align with
008 agent intentions. Section D experiment on alternative agent-
009 centric profiler baseline, confirming our proposed ACP’s
010 superiority in accuracy and collision metrics. Section E pro-
011 vides more qualitative analysis reflecting JACoP’s ability
012 to produce accurate, collision-free predictions in complex
013 scenes. Section F provide additional benchmark on SDD
014 dataset. Section G provides analysis on collision rate and
015 number of agent per scene.

016 A. Sampling Algorithm

017 Algorithm 1 details our proposed sampling algorithm,
018 which generates the scene prediction by aligning the pro-
019 totype trajectories selected by our Agent-Centric Profiler
020 (ACP). We employ Gibbs sampling, iteratively sampling a
021 trajectory for each agent conditioned on the trajectories of
022 all other agents from the previous sampling step. The pro-
023 cess is initialized by sampling from the marginal distribu-
024 tion inferred for each agent by the ACP module. We per-
025 form a total of $B + K$ iterations across all agents and retain
026 the samples from the final K steps as our set of scene pre-
027 dictions. This sampling procedure ensures that the samples
028 converge to the distribution defined by the Markov Random
029 Field (MRF) and the social filtering process, which is es-
030 sential for achieving realistic predictions with no social col-
031 lisions and high joint accuracy.

032 The sampling algorithm requires a time complexity of
033 $O(N(B + K))$, where the overall complexity grows lin-
034 early with the number of agents (N). We can further par-
035 allelize the sampling process by initializing K independent
036 processes, which allows the time complexity to be reduced
037 to $O(BN)$.

038 B. Evaluation Metrics

039 **Minimum ADE and FDE** The commonly used metric
040 $min_k ADE/FDE$ evaluates the average and final displace-
041 ment error of the most accurate sample among the multi-
042 modal prediction outputs. The ground truth future is de-
043 noted as $Y = \{Y_1, \dots, Y_n\}$, representing a scene compris-
044 ing multiple agents. Each agent’s trajectory is further de-
045 tailed as $Y_i = \{y_{i,1}, \dots, y_{i,T_f}\}$. The K prediction samples
046 are represented as $\hat{Y}^{(k)} = \{\hat{Y}_1^{(k)}, \dots, \hat{Y}_n^{(k)}\}$, with each

agent’s sample expressed as $\hat{Y}_i^{(k)} = \{\hat{y}_{i,1}^{(k)}, \dots, \hat{y}_{i,T_f}^{(k)}\}$, for
each $k = 1, \dots, K$. The metrics are defined as

$$min_k ADE(Y, \hat{Y}) = \frac{1}{TN} \sum_{i=1}^N \min_{k=1}^K \sum_{t=1}^T \|y_{t,i} - \hat{y}_{t,i}^{(k)}\|_2^2, \quad 047$$

$$min_k FDE(Y, \hat{Y}) = \frac{1}{N} \sum_{i=1}^N \min_{k=1}^K \|y_{T_f,i} - \hat{y}_{T_f,i}^{(k)}\|_2^2. \quad 048$$

049 **JADE/JFDE** The Joint Accuracy metrics, referred to
050 as JADE/JFDE, were initially introduced in [6] with
051 the objective of enhancing the widely used marginal
052 $min_k ADE/FDE$ metrics. These joint metrics are de-
053 signed to more accurately reflect a model’s capability to
054 predict the collective future trajectories of all agents present
055 within a given scene. Unlike the conventional approach,
056 which involves selecting each agent’s most accurate predic-
057 tion samples independently, JADE/JFDE calculates the av-
058 erage displacement error across all agents within a single
059 prediction sample. The JADE and JFDE are defined as
060

$$JADE(Y, \hat{Y}) = \frac{1}{TN} \min_{k=1}^K \sum_{i=1}^N \sum_{t=1}^T \|y_{t,i} - \hat{y}_{t,i}^{(k)}\|_2^2, \quad 061$$

$$JFDE(Y, \hat{Y}) = \frac{1}{N} \min_{k=1}^K \sum_{i=1}^N \|y_{T_f,i} - \hat{y}_{T_f,i}^{(k)}\|_2^2. \quad 062$$

063 **Agent-to-Agent Collision** The agent-to-agent collision
064 rate measures the proportion of predicted trajectories that
065 intersect with another agent’s path in the same scene predic-
066 tion. Two agents are considered to collide if their positions
067 come within $r = 0.2$ meters at any future time step. We
068 first define an indicator function for collision as
069

$$\mathbb{1}_{col}(\hat{Y}_i^{(k)}, \hat{Y}_j^{(k)}) = 1, \quad 070$$

$$\text{if } \exists t, \text{ such that } \|\hat{y}_{t,i}^{(k)} - \hat{y}_{t,j}^{(k)}\|_2 < r. \quad 071$$

072 Then we compute the agent-to-agent collision rate as

$$A2A_{CR} = \frac{1}{NK} \sum_{i=1}^N \sum_{k=1}^K \mathbb{1}_{col}(\hat{Y}_i^{(k)}, \hat{Y}_j^{(k)}), \quad 073$$

$$\text{for any } j, i \neq j. \quad 074$$

075 **Environmental Collision Rate** The environmental colli-
076 sion rate evaluates the percentage of predicted trajectories
077 overlap with non-navigable areas or environmental obsta-
078 cles. We first define an indicator function for environmental

Table 1. Average ADE/FDE and KDE-based NLL Benchmark. The best performance is boldfaced and the 2nd place is marked as blue.

Model	ETH	HOTEL	UNIV	ZARA1	ZARA2	ETH	HOTEL	UNIV	ZARA1	ZARA2
Avg. # Agents	2.6	3.5	25.7	3.7	6.3	2.6	3.5	25.7	3.7	6.3
Model	Average ADE/FDE					KDE NLL				
AgentFormer	1.99/4.39	0.87/2.01	1.01/2.26	0.72/1.63	0.74/1.71	2.70	1.60	1.88	1.52	1.53
GP-Graph	1.21/2.51	0.71/1.53	0.91/1.31	0.68/1.50	0.57/1.27	2.31	1.51	1.80	1.52	1.42
EqMotion	1.42/2.99	0.64/1.32	2.30/5.39	0.82/1.83	0.68/1.54	2.23	1.37	1.78	1.60	1.47
SingularTrajectory	1.47/2.77	0.89/1.88	1.12/2.36	0.92/1.96	1.02/2.23	2.04	1.58	1.93	1.67	1.77
JACoP	1.03/1.97	0.50/1.05	0.82/1.70	0.59/1.26	0.46/0.99	2.54	1.28	2.07	1.44	1.35

083 violations given the prediction $\hat{Y}_i^{(k)}$ and navigability map
084 M ,

$$086 \mathbb{1}_{env}(\hat{Y}_i^{(k)}, M) = 1, \text{ if } \exists t \text{ such that } M(\hat{y}_{t,i}) \neq 1. \quad (5)$$

087 Then we compute the proportion of predictions with envi-
088 ronmental violation via

$$089 ENV_{CR} = \frac{1}{NK} \sum_{i=1}^N \sum_{k=1}^K \mathbb{1}_{env}(\hat{Y}_i^{(k)}, M). \quad (6)$$

090 **Average ADE/FDE** Both the minimum k Average/Final
091 Displacement Error ($\min_k ADE/FDE$) and the Joint Av-
092 erage/Final Displacement Error (JADE/JFDE) primarily
093 evaluate prediction accuracy based on the best marginal or
094 joint sample. However, in a real-world deployment setting,
095 distinguishing the most accurate output from a set of model
096 predictions is impossible. Therefore, it is crucial that the
097 entire set of predicted futures does not deviate excessively
098 from the true trajectory. To better evaluate the model’s over-
099 all capability in producing realistic future predictions, we
100 propose the Average ADE/FDE as an additional accuracy
101 measure.
102

$$103 avgADE(Y, \hat{Y}) = \frac{1}{TNK} \sum_{i=1}^N \sum_{k=1}^K \sum_{t=1}^T \|y_{t,i} - \hat{y}_{t,i}^{(k)}\|_2^2,$$

$$104 avgFDE(Y, \hat{Y}) = \frac{1}{NK} \sum_{i=1}^N \sum_{k=1}^K \|y_{T,i} - \hat{y}_{T,i}^{(k)}\|_2^2. \quad (7)$$

105 The key difference between $\min_k ADE/FDE$ and
106 $avgADE/FDE$ lies in their aggregation strategy: instead
107 of selecting the best sample (i.e., the minimum error) from
108 the K outputs, $avgADE/FDE$ averages the displacement
109 error across all K model outputs. A smaller value for these
110 average metrics indicates that the model’s entire distribution
111 of predictions is tightly concentrated around the ground-
112 truth future.

113 **KDE-based NLL** To further examine the likelihood of
114 each method producing the ground-truth (GT) future among

all their prediction outputs, we benchmark the models using
the Kernel Density Estimation (KDE)-based Negative Log-
Likelihood (NLL) metric, as proposed in [3, 5]. The KDE-
NLL metric quantifies the probability density of the GT fu-
ture trajectory under a distribution inferred from the K pre-
dicted samples produced by the models. A smaller NLL
value indicates a tighter concentration of the model’s pre-
dicted distribution around the GT future, reflecting a more
accurate and confident overall prediction set. Here we use
Silverman’s rule of thumb to determine the optimal band-
width for the KDE estimation.

C. Average ADE/FDE and KDE NLL Analysis

Previous accuracy metrics primarily emphasize the model’s
best sample; this design was originally introduced to com-
pensate for the inherent stochastic nature of human trajec-
tory. While this metric effectively reflects the upper bound
of a model’s predictive capability, its optimization can inad-
vertently lead to models learning shortcuts. Specifically, a
model may produce highly diverse or scattered predictions
hoping that at least one sample happens to align closely with
the ground-truth future. Our previous benchmark results
have shown that state-of-the-art (SOTA) models, despite
their good accuracy upper bound, frequently produce highly
unlikely predictions that violate social and environmental
constraints. Consequently, these best-case accuracy mea-
sures become less convincing as a true indicator of model
quality.

To address this limitation, we introduce two additional
benchmark experiments to provide a more complete as-
sessment of the overall model capability for producing ac-
curate predictions. Specifically, we measure the Average
ADE/FDE and KDE-NLL of the model outputs, as pre-
sented in Table 6. Our JACoP model achieves a notable
improvement in Average ADE/FDE performance compared
with state-of-the-art (SOTA) methods. This suggests that
the model’s output distribution, on average, more closely
aligns with the ground-truth (GT) agent intentions.

To further support this finding, we evaluate the KDE-
NLL metric, which measures the likelihood of the GT fu-
ture trajectory under the sampling distribution of the model

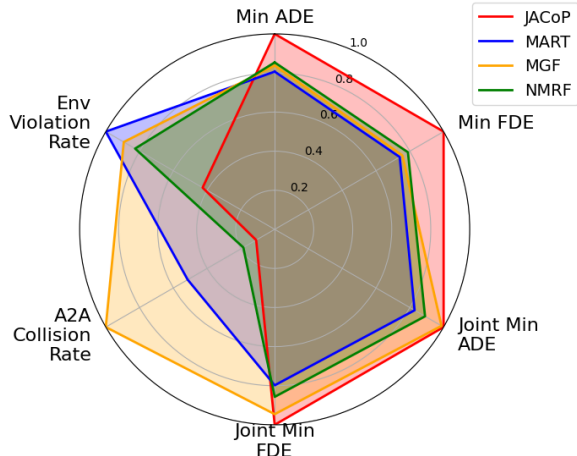


Figure 1. Radar Chart for normalized SDD evaluation result

Table 2. Accuracy and Collision Benchmark on SDD dataset. $\min_k ADE$ and JADE measured in pixel space. A2A collision threshold equals 5 pixels (roughly 0.2m). Best result in **bold face** and second best marked by **blue** color

Model	$\min_k ADE / \min_k ADE$	JADE/JFDE	A2A Collision	A2E Collision
MART	7.42/11.81	9.48/16.77	0.010	0.055
MGF	7.71/12.07	11.30/19.88	0.019	0.058
NMRF	7.86/12.59	10.19/18.02	0.004	0.066
Ours	9.20/15.97	11.45/21.02	0.002	0.028

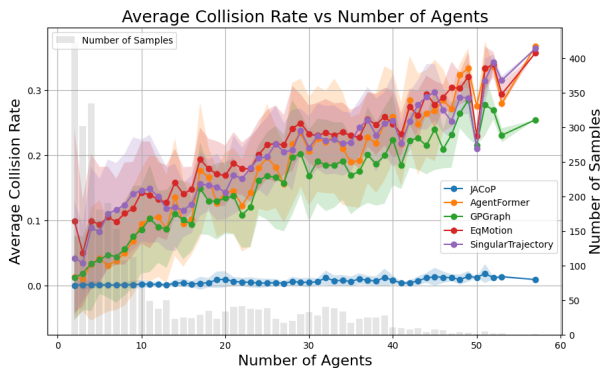


Figure 2. A2A collision rate versus number of agents on the ETH-UCY dataset, showing our JACoP model is clearly better at avoiding collisions, especially in crowded scenes.

155 outputs. Our model demonstrates strong performance relative to SOTA methods, particularly on the Hotel, Zara1, and
156 Zara2 splits, where JACoP sets a new performance benchmark.
157
158

159 Taken together, these results—combined with JACoP’s
160 ability to generate trajectories with minimal scene violations—support the conclusion that our JACoP model functions
161 as a reliable trajectory predictor capable of generating
162 multiple future possibilities that better reconcile both GT
163 agent intentions and environmental and social contexts.
164

D. Alternative Profiler Choice – AgentFormer 165

166 Our ablation study in Section 4.3 shows that the proposed
167 environmental and social collision filter and the Gibbs sam-
168 pling module are vital for generating collision-free scene-
169 level predictions. Given this result, we recognize that both
170 the filtering technique and our Joint Prediction Aligner
171 module (Figure 2, right) are generally applicable to other
172 Profiler modules, provided the module is probabilistic or
173 offers a scoring mechanism for trajectory proposals. How-
174 ever, we argue that our light-weight anchor-based Pro-
175 filer(ACP), which performs matching in the future trajec-
176 tory’s feature space, offers a sufficient and efficient solu-
177 tion. To further verify this hypothesis on the sufficiency of
178 our approach, we experimented with an alternative Profiler
179 choice, using the predictions and probability estimates from
180 AgentFormer [7] as inputs to our Joint Prediction Aligner.
181 We benchmark this alternative baseline against the original
182 AgentFormer and our proposed JACoP method.

183 Table 3, Table 4 and Table 5 show the performance on the
184 accuracy and feasibility benchmarks, while Figure 3 sum-
185 marizes the numerical results on the radar charts for better
186 head-to-head comparison. The results concerning environ-
187 mental and A2A collisions demonstrate that the combina-
188 tion of AgentFormer with our proposed aligner and filtering
189 technique (shown in blue polygon), significantly reduces
190 the collision rate compared to the original AgentFormer
191 (shown in green polygon). This robustly indicates the utility
192 and generalizability of the JACoP Aligner module.

193 However, the alternative AgentFormer Profiler fails to
194 outperform our anchor-based Agent-Centric Profiler (ACP)
195 (shown in orange) across the three main accuracy metrics,
196 KDE NLL and the A2A collision rate. Our utilization of
197 environmental and social contexts as part of the query em-
198 beddings helps the model select more accurate and suit-
199 able prototypes for subsequent alignment and scene pre-
200 diction generation. While the AgentFormer output shows
201 good performance in the best-case scenario (indicated by
202 the $\min_k ADE/FDE$ metrics), its inherent lack of envi-
203 ronmental awareness renders a majority of its predictions
204 unusable for alignment after the environmental filtering pro-
205 cess. The remaining filtered predictions, despite achieving
206 good environmental compliance, lack the necessary accu-
207 racy for the alignment process to produce a high-quality fi-
208 nal output, which also leads to more unavoidable social col-
209 lisions. The superior performance of JACoP in the average
210 ADE/FDE and KDE NLL further demonstrate that our pro-
211 posed ACP module helps the model achieve good average
212 accuracy across all selected samples and generate trajec-
213 tories that have a tight concentration around the GT future.

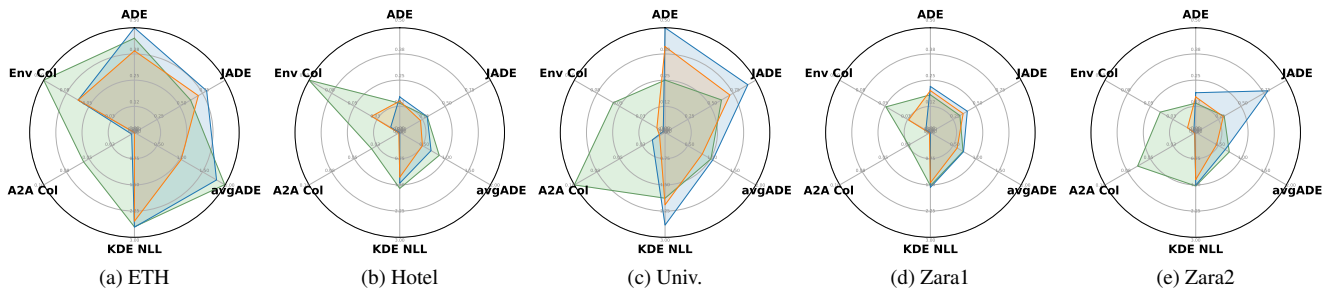


Figure 3. Radar plot for all metrics among the five ETH-UCY dataset splits comparing between AgentFormer+JACoP Aligner and JACoP. **Green: AgentFormer; Blue: AgentFormer Profiler + JACoP Aligner; Orange: JACoP.** A smaller overall area of the polygon aligns with better performance across all metrics.

Table 3. Collision Rate of our JACoP vs. AgentFormer + JACoP Aligner. The best performance is boldfaced and the 2nd place is marked as blue.

Model	ETH	HOTEL	UNIV	ZARA1	ZARA2	ETH	HOTEL	UNIV	ZARA1	ZARA2
Avg. # Agents	2.6	3.5	25.7	3.7	6.3	2.6	3.5	25.7	3.7	6.3
Model	Environmental Collision					A2A Collision				
AgentFormer	0.32	0.147	0.057	0.049	0.039	0.056	0.031	0.205	0.024	0.064
AgentFormer + JACoP Aligner	0.008	0.010	0.000	0.005	0.002	0.003	0.002	0.014	0.00	0.002
JACoP	0.062	0.031	0.009	0.024	0.009	0.00	0.001	0.006	0.001	0.001

214 E. Additional Qualitative Evaluations

215 We offer additional visualizations for qualitative analysis.
 216 Figure 4 presents examples of densely packed scenes, where
 217 our JACoP model accurately predicts without social or envi-
 218 ronmental collisions. For instance, row 2 depicts a crowd
 219 navigating dense areas. Compared to other SOTA mod-
 220 els, JACoP avoids agent collisions. It also provides accu-
 221 rate scene predictions, evident in the JADE performance for
 222 rows 1, 3, and 4.

223 Figure 5 illustrates individual predictions that demand
 224 a deep understanding of environmental constraints. Row
 225 1 features an ETH split example where the model pre-
 226 dicted a slowdown as the agent nears the scene’s edge. Our
 227 model, incorporating environmental context into the query
 228 embedding and filtering, generates trajectories that adhere
 229 to navigable areas and explores alternatives while respect-
 230 ing constraints. The SingularTrajectory model often fails
 231 due to post-prediction corrections, leading to infeasible pre-
 232 dictions. Other models, ignoring environmental contexts,
 233 tend to overshoot or overlap non-navigable areas. In two
 234 other instances, our JACoP models also achieve environ-
 235 mentally compliant predictions, especially in row 2, where
 236 our predictions align closely with the ground truth future.

237 F. Additional Benchmark – SDD

238 We added an SDD experiment comparing three SOTA mod-
 239 els: MART [4], MGF [1], and NMRF [2], summarized in the
 240 radar plot in Figure 1. Our model attains the best social and
 241 environmental collision rates—our main focus—with only

slightly lower accuracy. We will include full numerical re- 242
 sults in the final version. 243

G. Analysis on Collision Rate vs Number of 244 Scene Agent 245

246 We further showcase this robustness via the A2A collision 247
 rate (Fig. 2) across scenes of varying density, where our 248
 method decisively outperforms prior SOTA in generating 249
 feasible, collision-free predictions.

Table 4. Prediction Accuracy Comparison between our JACoP vs. AgentFormer + JACoP Aligner. The best performance is boldfaced and the 2nd place is marked as blue.

Model Avg. # Agents	ETH 2.6	HOTEL 3.5	UNIV 25.7	ZARA1 3.7	ZARA2 6.3	ETH 2.6	HOTEL 3.5	UNIV 25.7	ZARA1 3.7	ZARA2 6.3
Model	$\min_k ADE/FDE$					JADE/JFDE				
AgentFormer	0.45/0.79	0.14/0.22	0.25/0.45	0.18/0.30	0.14/0.23	0.619/1.136	0.303/0.603	0.622/1.311	0.325/0.660	0.314/0.663
AgentFormer + JACoP Aligner	0.52/0.94	0.17/0.29	0.62/1.29	0.22/0.43	0.19/0.37	0.796/1.572	0.303/0.614	0.912/1.942	0.407/0.869	0.372/0.807
JACoP	0.59/1.06	0.15/0.25	0.41/0.82	0.20/0.39	0.17/0.32	0.704/1.226	0.229/0.420	0.715/1.472	0.361/0.724	0.304/0.623

Table 5. Average ADE/FDE and KDE-based NLL Benchmark Comparison between our JACoP vs. AgentFormer + JACoP Aligner. The best performance is boldfaced and the 2nd place is marked as blue.

Model Avg. # Agents	ETH 2.6	HOTEL 3.5	UNIV 25.7	ZARA1 3.7	ZARA2 6.3	ETH 2.6	HOTEL 3.5	UNIV 25.7	ZARA1 3.7	ZARA2 6.3
Model	Average ADE/FDE					KDE NLL				
AgentFormer	1.99/4.39	0.87/2.01	1.01/2.26	0.72/1.63	0.74/1.71	2.70	1.60	1.88	1.52	1.53
AgentFormer + JACoP Aligner	1.81/3.92	0.69/1.56	1.05/2.26	0.73/1.65	0.65/1.48	2.71	1.45	2.65	1.57	1.51
JACoP	1.03/1.97	0.50/1.05	0.82/1.70	0.59/1.26	0.46/0.99	2.54	1.28	2.07	1.44	1.35

250

References

251
252
253
254
255
256
257
258
259
260
261
262
263
264
265
266
267
268
269
270
271
272
273
274
275
276
277
278

- [1] Jiahe Chen, Jinkun Cao, Dahua Lin, Kris Kitani, and Jiangmiao Pang. Mgf: Mixed gaussian flow for diverse trajectory prediction. *Advances in Neural Information Processing Systems*, 37:57539–57563, 2024. 4
- [2] Zilin Fang, David Hsu, Gim Hee Lee, and Gim Hee Lee. Neuralized markov random field for interaction-aware stochastic human trajectory prediction. In *ICLR*, 2025. 4
- [3] Boris Ivanovic and Marco Pavone. The trajectron: Probabilistic multi-agent trajectory modeling with dynamic spatiotemporal graphs. In *Proceedings of the IEEE/CVF international conference on computer vision*, pages 2375–2384, 2019. 2
- [4] Seongju Lee, Junseok Lee, Yeonguk Yu, Taeri Kim, and Kyooobin Lee. Mart: Multiscale relational transformer networks for multi-agent trajectory prediction. In *European Conference on Computer Vision*, pages 89–107. Springer, 2024. 4
- [5] Luca Anthony Thiede and Pratik Prabhanjan Brahma. Analyzing the variety loss in the context of probabilistic trajectory prediction. In *Proceedings of the IEEE/CVF International Conference on Computer Vision*, pages 9954–9963, 2019. 2
- [6] Erica Weng, Hana Hoshino, Deva Ramanan, and Kris Kitani. Joint metrics matter: A better standard for trajectory forecasting. In *Proceedings of the IEEE/CVF International Conference on Computer Vision*, pages 20315–20326, 2023. 1
- [7] Ye Yuan, Xinshuo Weng, Yanglan Ou, and Kris M Kitani. Agentformer: Agent-aware transformers for socio-temporal multi-agent forecasting. In *Proceedings of the IEEE/CVF International Conference on Computer Vision*, pages 9813–9823, 2021. 3

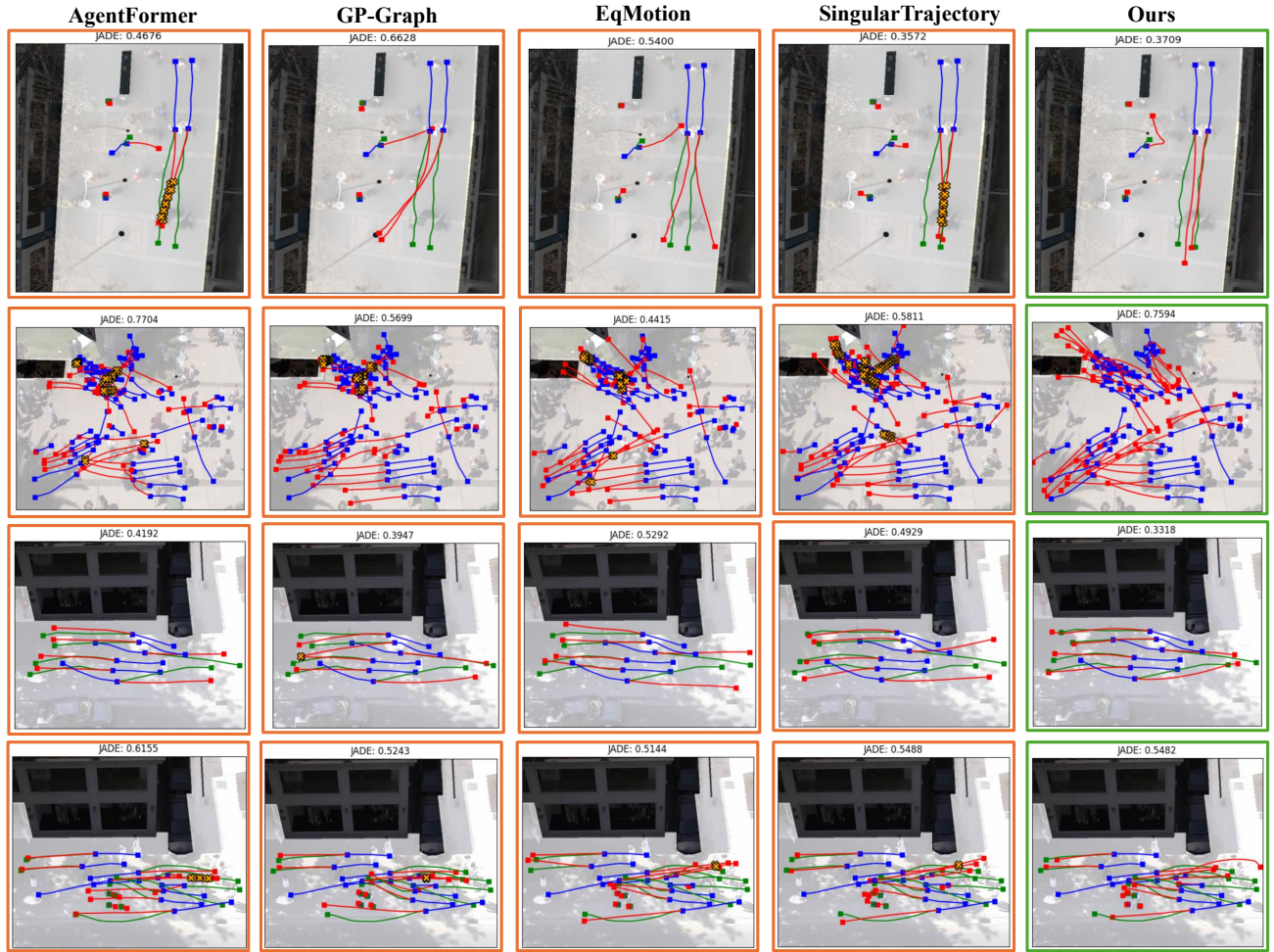


Figure 4. Scene prediction with best JADE performance from Hotel (Row 1), Univ (Row 2), Zara1 (Row 3) and Zara2 (Row 4)
Blue line: Historical Trajectory, Green line: Ground Truth Future Trajectory, Red line: Predictions.

Algorithm 1 Gibbs Sampling for Scene-Level Trajectory Prediction

Require: Number of burn-in steps B , number of samples K , and a set of agents \mathcal{I} .

Ensure: A set of scene predictions \mathcal{Y} .

```

1:  $Y^{(0)} \sim P_{\text{unary}}$  ▷ Initialize from marginal samples
2:  $\mathcal{Y} := \text{Empty List}$ 
3: for  $\tau = 1$  to  $B + K$  do
4:   for each agent  $i \in \mathcal{I}$  do
5:      $Y_i^{(\tau)} \sim P(Y_i | Y_{\setminus i}^{(\tau-1)})$  ▷ Sample agent  $i$ 's trajectory conditioned on all others
6:   end for
7:   if  $\tau > B$  then
8:     Append  $Y^{(\tau)}$  to  $\mathcal{Y}$  ▷ Save the scene prediction after burn-in
9:   end if
10: end for
    return  $\mathcal{Y}$ 

```

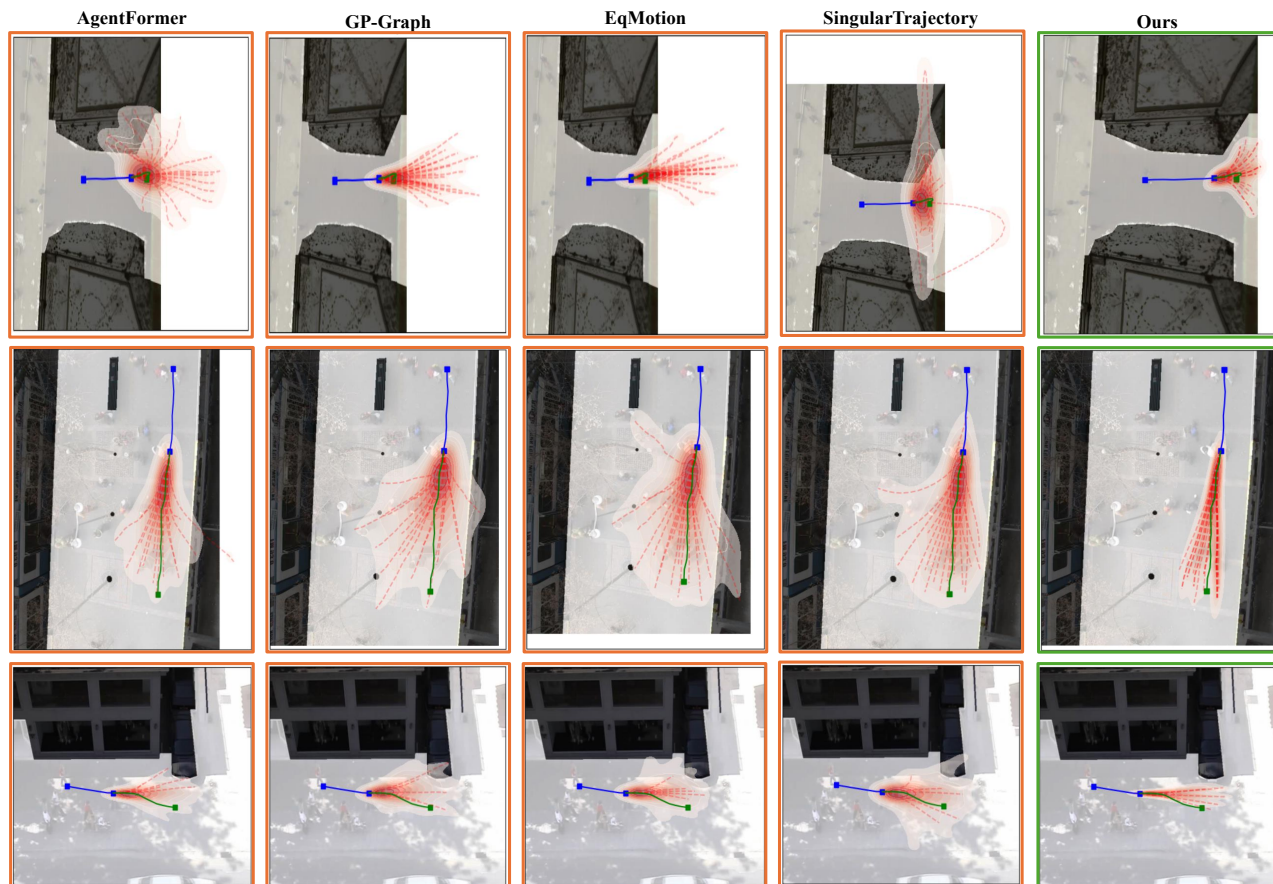


Figure 5. Individual prediction from ETH (Row 1), Hotel (Row 2) and Zara1 (Row 3)
Blue line: Historical Trajectory, Green line: Ground Truth Future Trajectory, Red Dashed line: Predictions, Red Shade: Sample Distribution.

Table 6. Average ADE/FDE and KDE-based NLL Benchmark. The best performance is boldfaced and the 2nd place is marked as blue.

Model	ETH	HOTEL	UNIV	ZARA1	ZARA2	ETH	HOTEL	UNIV	ZARA1	ZARA2
Avg. # Agents	2.6	3.5	25.7	3.7	6.3	2.6	3.5	25.7	3.7	6.3
Model	Average ADE/FDE					KDE NLL				
AgentFormer	1.99/4.39	0.87/2.01	1.01/2.26	0.72/1.63	0.74/1.71	2.71	1.35	1.72	1.30	1.29
AgentFormer + JACoP Aligner	1.81/3.92	0.69/1.56	1.05/2.26	0.73/1.65	0.65/1.48	2.81	1.19	2.93	1.38	1.29
GP-Graph	1.21/2.51	0.71/1.53	0.91/1.31	0.68/1.50	0.57/1.27	2.30	1.28	1.65	1.32	1.19
EqMotion	1.42/2.99	0.64/1.32	2.30/5.39	0.82/1.83	0.68/1.54	2.15	1.10	1.60	1.40	1.22
SingularTrajectory	1.47/2.77	0.89/1.88	1.12/2.36	0.92/1.96	1.02/2.23	1.91	1.34	1.77	1.46	1.57
JACoP	1.03/1.97	0.50/1.05	0.82/1.70	0.59/1.26	0.46/0.99	2.76	1.01	2.10	1.24	1.12